Exploring the Effects of Cell-to-Cell Variability on Battery Aging through Stochastic Simulation Techniques

Elias Barbers[1,2,3,z], Friedrich Emanuel Hust[2], Felix Emil Arthur Hildenbrand[2,3], Fabian Frie[2,3], Katharina Lilith Quade[2,3], Stephan Bihn[2,3], Dirk Uwe Sauer[2,1,3] and Philipp Dechent[2,3,z]
[1]Helmholtz Institute Münster (HI MS), IEK-12, Forschungszentrum Jülich, Campus Boulevard 89, 52066 Aachen, Germany
[2]Institute for Power Electronics and Electrical Drives (ISEA), RWTH Aachen University, Aachen, Germany
[3]Jülich Aachen Research Alliance, JARA-Energy, 52425 Jülich, Germany
[z]Corresponding Authors: Elias Barbers e.barbers@fz-juelich.de, Philipp Dechent philipp.dechent@googlemail.com

Abstract

This work introduces a comprehensive modeling framework designed to simulate the electrical, thermal, and aging behavior of battery cells connected in various parallel and series configurations. By utilizing Monte Carlo simulation techniques, the framework is used to investigate the inherent variability in cell attributes, including initial capacity, aging rate, and application profiles. Besides the estimation of expected battery life, this simulation environment enables the detailed investigation of failure distributions across different cell configurations and intensities of parameter variations. Results obtained from these simulations can be used, as an example, in the context of the automotive industry, where the insights of simulation in understanding the inherent variability of the aging process are particularly vital. As electric vehicles become more prevalent, understanding the performance and longevity of battery packs under various conditions is essential for effective design and management strategies, optimizing vehicle range, safety, and cost-effectiveness also on a fleet-level. Moreover, the ability to investigate failure distributions provides invaluable information for improving battery reliability and safety, key factors in the consumer acceptance of electric vehicles. Ultimately, the simulation environment provides a powerful tool for designing and optimizing efficient and durable battery technologies, with a focus on failure distribution analysis.

Introduction

Lithium-ion batteries are at the core of numerous applications ranging from home storage systems to grid storage systems, but the most significant driver of battery growth is the automotive industry. The surge in electric vehicle production is expected to increase battery production capacity by several hundred gigawatt-hours per year. However, not all batteries are created equal, and variances in cell properties can significantly affect battery performance

and lifespan [1]. To optimize battery design and minimize costs, it is imperative to understand and account for these variances.
For instance, the parameters of initial capacity and resistance, which are recorded during production, can be used for a preselection of battery cells. While tighter margins may ensure higher quality, they also result in a higher rejection rate, increasing the overall cost of production. Therefore, the key to cost-effective battery pack production does not solely lie in narrowing these margins, but also in effectively managing them.

Optimal system design doesn't solely rely on minimizing the risk of battery function loss; it also necessitates a careful cost-benefit analysis, especially regarding warranty-related battery replacements. This consideration can vary significantly based on the application. An example is micro mobility and shared electric scooters, where feasible battery replacement strategies can reduce the number of cells that have to be discarded during the manufacturing process. Consequently, even though it may increase the rate of battery failures, allowing for a slight increase in aging rate variability could be a cost-effective choice.
Achieving the best outcomes requires a balanced view. We must consider not just the ideal product from an engineering standpoint, but also the challenges introduced by uneven production. Therefore, simulation tools that account for cell-to-cell variability are crucial for designing battery systems that minimize total ownership costs.
Battery topology, another crucial variable of battery design, can vary significantly between different automotive applications. For example, there are commercial cells like the BYD Blade, which uses a single cell of over 200Ah, and others like earlier versions of the Model S 100kWh battery that employs 86 smaller cells in parallel. In between these extremes, there are various configurations like the Model Y 4860, which uses nine medium-sized cells, as well as many designs with two or three cells in parallel.
Another noteworthy aspect is the fit of the operating strategy. A poor fit, leading to suboptimal battery performance, could result from a discrepancy in the current reading due to cheaper measurement technology or poor battery state estimation. Understanding and addressing such factors can further enhance battery performance and lifespan.

In this light, a stochastic aging model that incorporates the statistical spread of parameters from cell to cell can be a valuable tool. This model can simulate variances in initial parameters, aging rates, and usage patterns across different battery systems and topologies. Moreover, it can simulate fleet-level failure rates as well as single-cell failures within a battery, providing a holistic understanding of battery performance and lifespan.
Current research efforts have begun to address the issue of cell-to-cell variability in lithium-ion batteries. For example, Reniers et al. [8] simulated individual cells and components of a grid storage system to quantify the impact of cell-to-cell variability. However, their model, while physics-based, did not fully account for varying aging rates and their impact on cell and pack lifetime. Similarly, the work by Dubarry et al. [9] also contributed to the understanding of cell-to-cell variabilities but lacked an aging model directly influenced by usage scenarios.
Paul et al. [3] utilized a thermal electric aging model and the Monte Carlo method to account for cell aging discrepancies within a battery system due to temperature and production variances. Zhang et al. [10] innovated an approach independent of offline training data to predict battery life, leveraging Monte Carlo simulation to manage uncertainties. Fill et al. [11] examined the effects of cell-to-cell variances on battery aging by coupling an Equivalent Circuit Model (ECM) with a thermal and aging model, and performing Monte Carlo simulations. These investigations highlight the need for a comprehensive tool to simulate cell-to-cell variability

and to use Monte Carlo methods in battery performance analysis, which our proposed stochastic aging model aims to offer.
All these studies underscore the need for a model that can accurately simulate cell-to-cell variances, incorporate different aging rates, and predict their impact on battery performance and lifespan over time.

This paper presents a novel stochastic aging model that captures these complexities. By using a Monte Carlo approach, we simulate the impact of variations in cell capacity, aging rate, usage profile, and battery topology on overall system performance. Our aim is to provide a comprehensive simulation tool that can guide cost-effective battery design and production strategies, ultimately improving the total cost of ownership for various applications, with an exemplary focus on the automotive sector. With this tool we strive to answer the following questions: How does initial cell-to-cell variation, cell aging rate variation, and usage variation impact the degradation of lithium-ion battery packs, and how can this understanding be used to optimize the design and topology for improved performance on a fleet level? Furthermore, how does the pack topology affect the level of variation between cells that is acceptable for the application, and how can this knowledge be used to find a tradeoff between high quality cells and cost-effective battery packs?

Simulation Framework

The simulations in this work are carried out within the simulation framework ISEAFrame, which is publicly available online [12]. It provides a simulation environment for lithium-ion batteries and is implemented in C++. The simulation framework is shown in Fig. 1 and consists of an electrical, a thermal, and an aging simulation. The three models are executed in a closed loop and exchange data throughout the simulation, which is used to update the electrical model during the simulation. The framework can be used to simulate single cells or whole battery packs with interconnected cells over time periods ranging from seconds to multiple years [13], [14]. The individual models and their interactions are described in the following paragraphs.

To start a simulation, besides a current or power profile, a model parameter file is needed as an input describing the model that is used. It contains the topology of the equivalent circuit for the electrical simulation as a tree-like structure, in which one element can contain several child elements. For example, a parallel circuit contains the individual elements connected in parallel as children. In addition, thermal blocks with specified material properties are assigned to the simulated cells to describe the thermal behavior of the battery. If an aging model is used, each cell is assigned a list of aging effects.

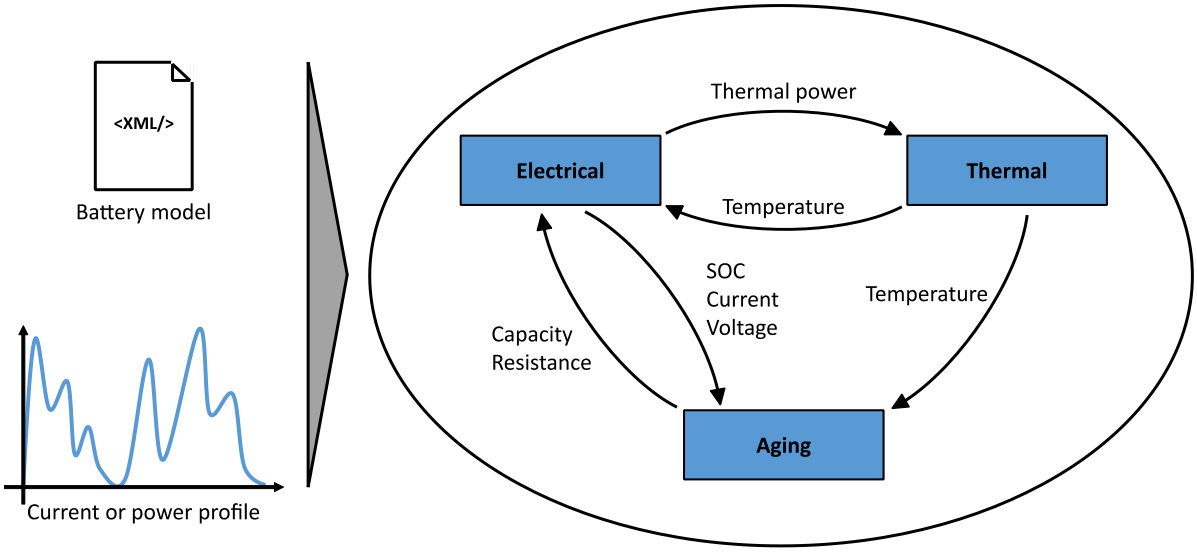

Figure 1: Overview of the combined electric, thermal and aging simulation.

Multiple cells in various pack topologies can be simulated by combining multiple equivalent circuits in a parallel or series connection. In this case, the values for temperature and the State-of-Charge (SOC) are treated separately for each cell. The simulation takes the current applied to the entire battery and calculates the current distribution over the individual cells.

Electrical model

The electrical behavior of a cell is simulated using an ECM with the structure depicted in Fig. 2 The ECM components depend on the SOC and the temperature and are parameterized by lookup tables. These tables are constructed based on the fitting of measurement data obtained from current pulses conducted at various SOCs and temperatures, as well as electrochemical impedance spectroscopy (EIS) measurements. [15] Each capacitor in the ECM introduces a differential equation. Parallel connections in the ECM lead to linear equations which results in a differential-algebraic system of equations that is transformed into an ordinary differential equation system and solved.

This electrical model is then used to simulate the electrical response of a battery to a current that is applied. It calculates the resulting battery voltage, the change in SOC and the heat that is generated by ohmic losses. The generated heat is passed to the thermal model (see Fig. 1), where it is used to calculate the temperature of each simulated battery cell. The temperature values are returned to the electrical model and used to update the temperature-dependent parameters of the ECM.

To perform the aging simulation in a reasonable time, it is necessary to find a good trade-off between the accuracy of the electrical model and the computational complexity. Therefore, the choice of ECM is highly dependent on the application. From highly sophisticated physically motivated ECMs to simple RC-element models, the complexity and the computational effort decreases as fewer ECM-elements need to be calculated. The best compromise to perform the stochastic aging simulation is a Thévenin-based model, consisting of a voltage source representing the open circuit voltage (OCV) as well as a serial resistor and two RC circuits. The serial resistance represents the instantaneous voltage drop caused by a charging or discharging current, while the RC circuits, consisting of a parallel connection of a resistor and

a capacitance, represent the transient behavior under load, but also during relaxation when no current is applied to the battery. The first RC circuit models the overvoltages caused by the double layer capacitances and charge transfer resistances of both electrodes, while the second RC circuit combines the migration and diffusion processes within the electrodes and the electrolyte. Such simplified models are often used for aging simulation at the pack level as well as at the cell or module level. [16], [17]

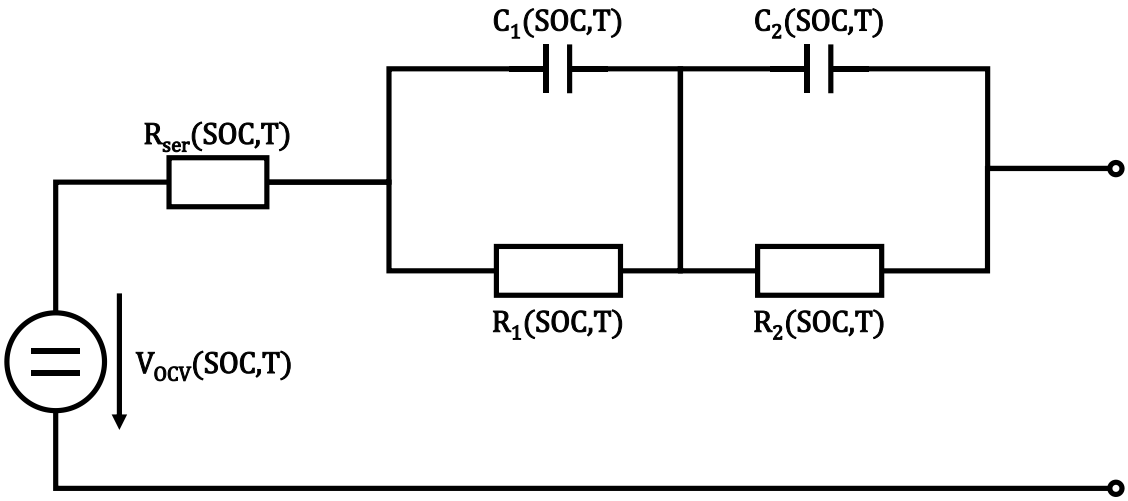

Figure 2: Representation of the used equivalent circuit model according to Thévenin.

A hybrid approach combining measurement data from the frequency domain and the time domain was used to obtain the best-fit parameter set. While R_{ser} is parameterized using impedance data from electrochemical impedance spectroscopy, the two RC circuits are fitted to pulse measurements in the time domain. For the time domain fitting, the voltage of the measurement is reduced by the OCV and the voltage drop caused by the already parameterized R_{ser}. This process is done for different points with respect to temperature and SOC and the resulting lookup table for every parameter is part of the electrical model used in the simulation. The model used in this work has been derived for an NCA type cell with a nominal capacity of 3.015 Ah. It has been validated to measurements of pulses with different C-rates and to drive cycles.

To simulate a battery pack, the ECM for a single cell can be repeated in parallel or series configurations. Additionally, a resistance is inserted between connected cells to account for wiring resistances. The detailed parameterization of the electrical model is available in the Supplementary Information.

Thermal model

The temperature of the battery is an important parameter for the simulation, as it affects both the electrical behavior and the aging that occurs. A thermal model is required to calculate the temperature based on the ambient temperature and the heat calculated as part of the electrical model. The model used in this work is based on the finite volume method. Here, the simulated space is divided into small thermal elements, each of which is assumed to have a uniform temperature. It is parameterized with the heat capacity and thermal conductivity of the simulated materials, where the thermal conductivity can be different for each dimension. Using

the thermal material properties, the heat flow between each pair of adjacent volumes can be calculated as a function of the difference between their temperatures. This results in a system of differential equations that is used to calculate the temperature of all volumes.
The temperature values calculated in the thermal model are fed back into the electrical model and used to update the parameters of all temperature-dependent components in the equivalent circuit. For this purpose, the temperature values of all thermal volumes within one battery cell are averaged. The combination of electrical and thermal simulation is necessary to provide greater accuracy, especially at higher currents that lead to self-heating of the battery.
A detailed thermal model typically consists of a large number of thermal volumes, which significantly increases the required computation time. Therefore, the required accuracy of the thermal model must be balanced against the increase in simulation time.

For this model, no thermal measurements were performed; instead, the following values from [18] within the normal range for cylindrical cells were used (density $2700\,\frac{kg}{m^3}$, heat capacity $1000\,\frac{J}{kg \cdot K}$, thermal conductivity in-plane $30\,\frac{W}{m \cdot K}$, thermal conductivity through-plane $1\,\frac{W}{m \cdot K}$). The thermal model was configured to use 64 thermal elements for each simulated cell, with 8 divisions in the height dimension and 8 divisions in the phi dimension. The ambient temperature was set to 20 °C.

The electrical and thermal simulations are performed alternately, creating a cycle by exchanging thermal power and temperature. The process begins with the electrical simulation, which executes incremental time steps until either a change in current occurs or a predefined maximum time (10 seconds in our simulations) has passed. Subsequently, the same time span is simulated thermally. This portion is also divided into multiple smaller time steps for more precise modeling. If at any point during these thermal steps a temperature difference threshold of 10 Kelvin is exceeded, the simulation process reverts back to the electrical simulation, specifically to the time step where the threshold was breached.
After each time step, the SOC of all cells is updated. This is done by multiplying the current through each cell by the duration of the time step to determine the amount of charge by which the SOC has changed. With the changed values for SOC and temperature, the component values of the ECM are updated after each time step.
The simulation framework can also be used for a half-cell simulation where separate ECMs are used for the anode and cathode. The OCV of the cell is then replaced by a voltage source in each of the two electrodes, which represents the potential of the electrode and from which the cell voltage is obtained. In the half-cell simulation, the anode, cathode, and entire cell have individual SOCs, which are calculated separately.

Aging model

An aging model is used to simulate the decrease in capacity and increase in internal resistance of the battery over time based on the operating conditions of the battery. It models irreversible changes in the battery that modify its electrical behavior and depend on the operating conditions. The function and parameters of the battery are predicted by the aging model from specific stress factors. Aging models for lithium-ion batteries vary in their level of abstraction. In basic terms of Failure Mode and Effects Analysis, these levels are classified as effect level,

mode level and mechanism level [19]. The highest level, effect level, is the observable states of capacity fade and internal resistance rise or power fade.
For more detail, capacity fade is subdivided into modes, on the one hand, the irreversible Loss of Lithium Inventory and Loss of Active Material [19] and on the other hand, reversible modes such as homogeneity of lithium distribution or the passive anode effect [20]. For even a greater detail level, individual degradation mechanisms can be modeled with their cause as input [21]. More detailed models allow a better understanding of the failure modes and probabilities, but are dependant on more complex characterization measurements and
further increase the computational complexity. For example, to parameterize the passive anode overhang model, cells must be disassembled and the electrode dimensions precisely determined.

In this work, a semi-empirical effect aging model based on Schmalstieg et al. [22] is used. The model has been implemented in the simulation framework and is used in combination with the electrical and thermal models [14]. Stress factors are accumulated during the simulation and used to update the battery parameters at certain time intervals. These intervals must be strategically chosen to ensure that degradation-relevant events within a given timeframe aren't overlooked, while simultaneously aiming to minimize computational effort.
To parameterize the aging model, aging tests are performed in which cells are aged under constant conditions in order to investigate the influence of these conditions on the rate of aging. Aging tests can be divided into calendar and cycle tests. In a calendar test, the cell is aged at a constant SOC and temperature. In a cycle test, the cell is subjected to continuous charging cycles. The temperature, depth of discharge, average SOC and current are kept constant. This is used to determine the aging that occurs in addition to the calendar aging when the cell is actively used.
By aging multiple cells at different conditions, such as different temperatures and different (mean) SOCs, a test matrix is created with aging data at different points. This makes it possible to create an aging model that calculates the aging of a cell as a function of the above parameters. This testing process is described in detail in the literature [23]–[25].

The semi-empirical aging model does not model the chemical processes within the battery, but rather finds mathematical functions that describe the aging of the battery. Individual aging processes, such as SEI growth, are not directly modeled. Instead, only the effective changes in capacity and resistance that directly affect the electrical behavior of the entire battery are modeled. These changes are described as functions of time, temperature, SOC, DoD, and charge throughput [22]. For example, elevated temperatures and high SOCs induce a high aging rate. Fig. 3 shows a schematic of the model based on Ecker and Schmalstieg [22], [26]. The model is divided into a cycle and a calendar aging part. The calendar aging is independent of usage and modeled dependent on SOC, temperature and cell age. The cycle aging that occurs due to the usage of the battery is modeled based on the charge rate, the cycle depth and the average SOC of the battery during operation.

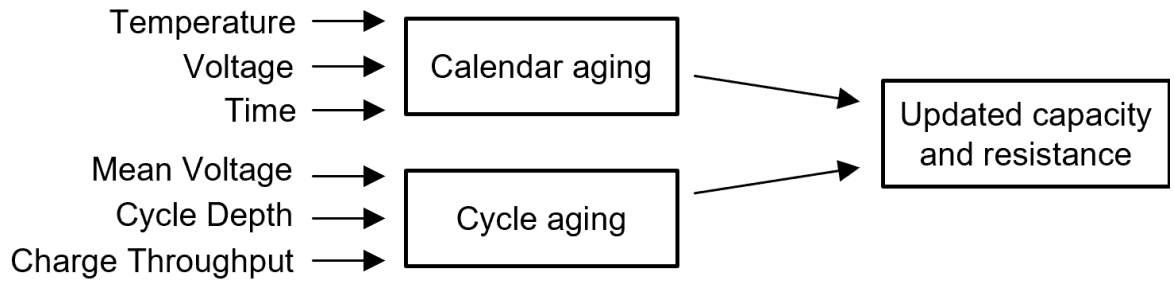

Figure 3: Structure of semi-empirical effect aging model from Schmalstieg et al.

To calculate the calendar aging, the model uses the aging factors α_{cap} and α_{res}. The original model described by Schmalstieg et al. provides equations that assume constant stress factors throughout the life of each cell. For the aging model, an iterative version of these equations is required, so that the relative capacity $C_{cal,i}$ and the relative resistance $R_{cal,i}$ after the ith aging step can be calculated based on the previous values $C_{cal,i-1}$ and $R_{cal,i-1}$ according to the following formulas:

$$C_{cal,i} = 1 - ((1 - C_{cal,i-1})^{\frac{1}{0.8}} + \Delta t \cdot \alpha_{C,i}^{\frac{1}{0.8}})^{0.8}$$

$$R_{cal,i} = 1 - ((1 - R_{cal,i-1})^{\frac{1}{0.8}} + \Delta t \cdot \alpha_{R,i}^{\frac{1}{0.8}})^{0.8}$$

The stress factors α_{cap} and α_{res} include the dependence of aging on SOC and temperature. Their value can be determined individually for each cell by fitting a function through the cell's measured capacity and resistance values. This gives values for the aging factors at the individual points of the test matrix. Subsequently, the voltage and temperature dependence can be determined by fitting an equation of the form

$$\alpha = (\alpha_1 + \alpha_2 \cdot SOC) \cdot e^{\frac{\alpha_3}{T}}$$

The cycle aging factors are not calculated as a function of time, but of the previous charge throughput:

$$C_{cyc,i} = 1 - ((1 - C_{cyc,i-1})^2 + \Delta Q \cdot \alpha_{C,i}^2)^{0.5}$$

$$R_{cyc,i} = 1 - ((1 - R_{cyc,i-1}) + \Delta Q \cdot \beta_{R,i})$$

The factor β depends on the DOD and the mean SOC. Before it is determined from the measured data of the aging tests, the calendric aging calculated by the model is subtracted from the data so that only the cyclical aging remains. β_{cap} and β_{res} are fitted to the equation

$$\beta = b_1 \cdot (\underline{SOC} + b_2)^2 + b_3 \cdot DOD + b_4$$

Monte Carlo simulation

Monte Carlo simulations are a method of simulating complex statistical processes that allows one to estimate the outcome distribution of a random process when the closed form of the distribution is unknown. A random number generator is used to randomly vary one or more parameters of a simulation. The simulation is run repeatedly with different values, producing different results. The data generated can be analyzed to see how the variation of a parameter affects the model.

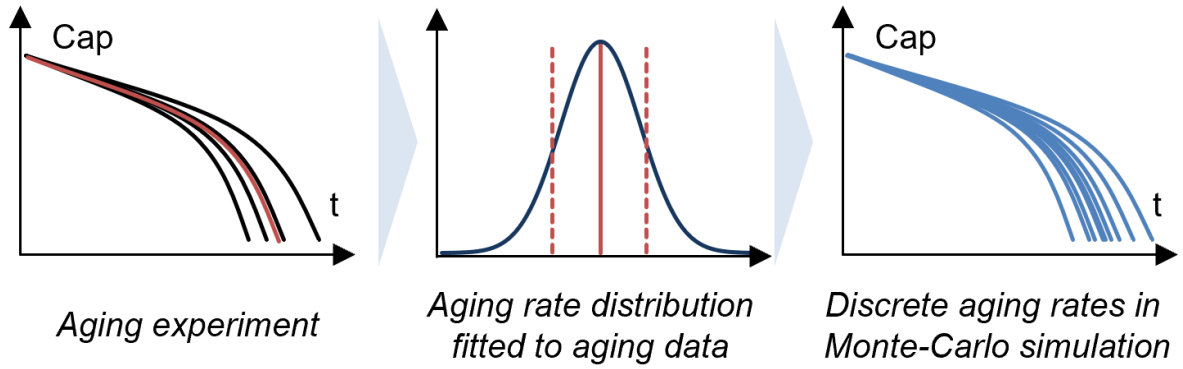

Figure 4: From aging experiments, an aging rate distribution is derived and used to create random aging rates for the Monte Carlo simulation. The mean of the aging rate distribution is marked in red and also shown as the fit of the curves in the aging experiment.

A normal distribution is often used for this purpose and it has been shown that parameters such as the initial capacity and internal resistance of battery cells follow normal distributions [4]. In addition Weibull distributions were proposed before and could be simulated as well, since the Weibull distributions also account for early failures [27]. During aging, the standard deviation of the cell parameter distributions may increase [28]. Also, the results of Monte Carlo simulations often follow a normal distribution. To determine the underlying distribution from the values of a simulated quantity that is assumed to be normally distributed, probability density estimation can be used to estimate the mean value and standard deviation of the normal distribution that is most likely to produce the observed samples.

Monte Carlo simulations can be performed with the presented battery model to simulate the influence of parameter variations on the degradation of battery cells and packs. The aging of batteries can be regarded as a statistical process, in which the aging rate of individual cells varies and results in different capacity trends as illustrated in Fig. 4.
In the simulation, a difference in initial parameters between two cells results in differences in electrical behavior that affect the entire simulation, including the calculated aging rate. When simulating a battery pack, differences in electrical behavior lead to uneven current distribution between cells, which introduces additional variance.

To obtain reliable results using the Monte Carlo method, a large number of simulations is required to obtain statistically significant results. If too few simulations are performed, the given variation of parameters cannot be generated accurately enough, causing a statistical error in the result. This effect can be observed by using a normal distribution to generate a number of samples and then using probability density estimation to estimate the parameters of the resulting distribution. For small sample sizes, the parameters of the estimated distribution may have a large deviation from the original distribution parameters. Therefore, to obtain reliable

results, all simulations in this paper were performed 100 times. All simulated packs contain at least 100 cells each, resulting in at least 10.000 simulated cells for each parameter variation.

Simulations

To conduct stochastic simulations using the model described above, parameters must be chosen that are varied according to a probability distribution. The parameters chosen for this work are the initial cell capacity, the aging rate, and the intensity of the application profile. Additionally, three different topologies were investigated.

An overview of all simulation campaigns is given in Table 1. For all simulations, the aging of the cells is simulated at constant cycling for 300 days. An aging step, in which the capacity and resistance of the cells are updated, was performed every 10 days. Before each aging step, the model is simulated once electrically and thermally with the given current profile. In the aging step, the stress factors for aging are calculated from this and used for the entire 10-day period. Thus, only one cycle is simulated and then it is assumed that the cell is cycled at identical conditions for the rest of the time.

For load profiles in addition to simple constant current cycling, more complex profiles, for example, the Worldwide harmonized Light vehicles Test Procedure (WLTP), are used. A current profile based on this test procedure is used for the simulations described in this work. Since the WLTP only defines a target velocity, a real vehicle or full vehicle model is necessary to determine the power demand. The model used to create current profiles in this work is described in [29], [30] and uses a full vehicle model including a driver model, drive train, aerodynamics, power electronics as well as a battery system. The current profile is scaled for each topology such that the maximum DOD for a cell with nominal capacity is 20%. In each individual simulation, 100 cells are simulated.

Normal distributions with standard deviations of 3 and 5 % were used for all parameter variations that were simulated. A detailed description of cell-to-cell variation can be found in [2]. Initial cell variations are on the upper bounds of [3]–[5] and the spread of aging rates from [6], [7]. For the initial cell capacity, the value for each individual cell is set according to the probability distribution with the nominal capacity as the mean value.

To vary the aging rate of the simulated cells, the coefficients in the equation for the cycling aging stress factor β are varied. The aging function contains coefficients that describe the dependence of the aging rate on the parameters temperature and SOC for calendric aging, and DOD and average SOC for cyclic aging. Each of these coefficients can be varied in order to simulate a variability in aging rate between multiple cells. As with the other varied parameters, a normal distribution was used to determine values for each simulated cell. The coefficients are varied independently from each other.

To investigate the effect of the variability of different usage scenarios on the aging, the entire current profile is multiplied by a factor drawn from a probability distribution. Since the current is always specified for the entire battery pack, all cells of a pack were always cycled with the same current and differ only by their capacity.

No.	Topology	Initial Capacity	Aging Rate	Application Profile
1	100s1p	Normal dist. ($\mu = 3\%$)	uniform	uniform
2	100s1p	Normal dist. ($\mu = 5\%$)	uniform	uniform
3	100s1p	uniform	Normal dist. ($\mu = 3\%$)	uniform
4	100s1p	uniform	Normal dist. ($\mu = 5\%$)	uniform
5	100s1p	uniform	Uniform	Normal dist. ($\mu = 3\%$)
6	100s1p	uniform	Uniform	Normal dist. ($\mu = 5\%$)
7	100s1p	Normal dist. ($\mu = 3\%$)	Normal dist. ($\mu = 3\%$)	Normal dist. ($\mu = 3\%$)
8	100s1p	Normal dist. ($\mu = 5\%$)	Normal dist. ($\mu = 5\%$)	Normal dist. ($\mu = 5\%$)
9	50s2p	Normal dist. ($\mu = 3\%$)	Normal dist. ($\mu = 3\%$)	Normal dist. ($\mu = 3\%$)
10	20s5p	Normal dist. ($\mu = 3\%$)	Normal dist. ($\mu = 3\%$)	Normal dist. ($\mu = 3\%$)
11	100s10p	Normal dist. ($\mu = 3\%$)	Normal dist. ($\mu = 3\%$)	Normal dist. ($\mu = 3\%$)
12	100s10p	Normal dist. ($\mu = 5\%$)	Normal dist. ($\mu = 5\%$)	Normal dist. ($\mu = 5\%$)
13	100s1p	Normal dist. ($\mu = 0.5\%$)	Normal dist. ($\mu = 0.5\%$)	Normal dist. ($\mu = 0.5\%$)
14	100s1p	Normal dist. ($\mu = 1\%$)	Normal dist. ($\mu = 1\%$)	Normal dist. ($\mu = 1\%$)
15	100s1p	Normal dist. ($\mu = 1.5\%$)	Normal dist. ($\mu = 1.5\%$)	Normal dist. ($\mu = 1.5\%$)
16	100s1p	Normal dist. ($\mu = 2\%$)	Normal dist. ($\mu = 2\%$)	Normal dist. ($\mu = 2\%$)
17	100s1p	Normal dist. ($\mu = 2.5\%$)	Normal dist. ($\mu = 2.5\%$)	Normal dist. ($\mu = 2.5\%$)
18	100s1p	Normal dist. ($\mu = 3\%$)	Normal dist. ($\mu = 3\%$)	Normal dist. ($\mu = 3\%$)
19	100s1p	Normal dist. ($\mu = 3.5\%$)	Normal dist. ($\mu = 3.5\%$)	Normal dist. ($\mu = 3.5\%$)
20	100s1p	Normal dist. ($\mu = 4\%$)	Normal dist. ($\mu = 4\%$)	Normal dist. ($\mu = 4\%$)
21	100s1p	Normal dist. ($\mu = 4.5\%$)	Normal dist. ($\mu = 4.5\%$)	Normal dist. ($\mu = 4.5\%$)
22	100s1p	Normal dist. ($\mu = 5\%$)	Normal dist. ($\mu = 5\%$)	Normal dist. ($\mu = 5\%$)

Table 1: Overview of conducted simulations

Results & Discussion

Variability of the initial capacity

First, the effect of a variability of the initial capacity on the aging of the cells is investigated. This variability causes the DOD to differ from cell to cell for the same current profile and thus

affects the aging. In the case of purely calendar aging without cycling of the cells, this effect does not exist, since aging depends only on SOC and temperature.

During the manufacturing process of lithium-ion batteries, initial capacity and resistance are key parameters that are recorded for each cell. These parameters are crucial as they provide essential information about the cell's potential performance and longevity, allowing manufacturers to preselect and group cells with similar characteristics for specific applications. This preselection process significantly influences the overall initial parameters of the cells in the application, leading to a more uniform and predictable battery performance and lower variability.

Tighter margins mean a more stringent selection process, leading to a higher rejection rate of cells that don't meet the set criteria. This not only increases the production cost due to a higher percentage of discarded cells, but also creates potential issues with production efficiency and material waste. Manufacturers then face a trade-off between the quest for optimal cell uniformity and the economic impact of a high rejection rate.

The effect of a variation in initial capacity was simulated in simulations 1 and 2. Because of the series connection, the current through each cell always has the specified value of the current profile. The capacity of each cell has been varied around the nominal value with a standard deviation of 3% and 5%.

The distribution of the capacity at the beginning of the simulation and during the simulation is shown in Fig. 5. It can be seen that the distribution of the cell capacities follows a normal distribution at every point during the simulation. The standard deviation of this distribution increases during the simulation as cells with lower capacity are subject to higher cycle depths and thus age more quickly.

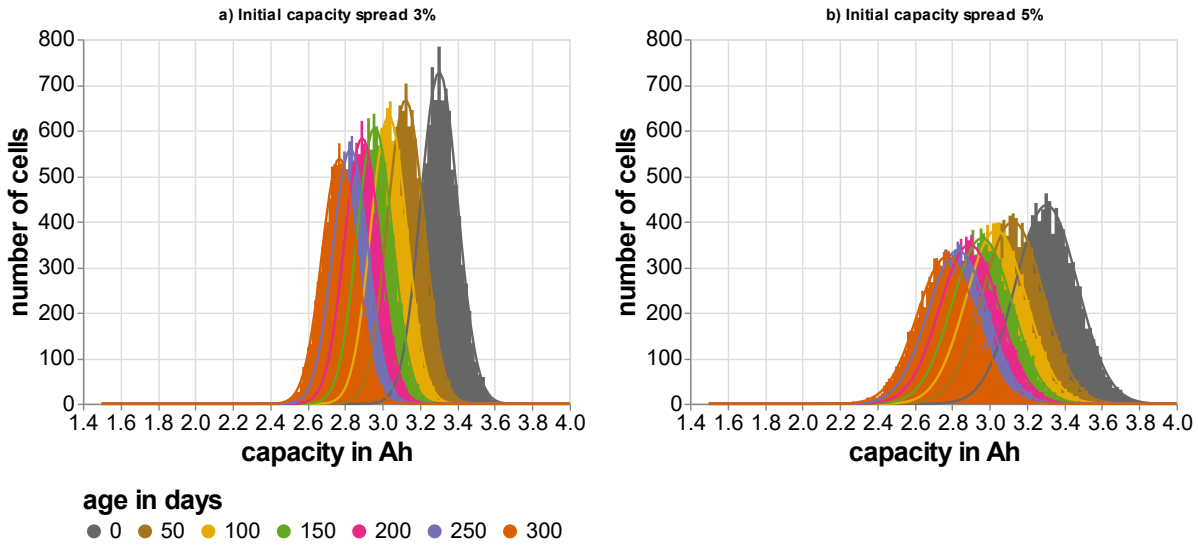

Figure 5: Evolution of the distribution of cell capacity during aging with a variability of initial capacity. a) Simulation 1 b) Simulation 2

Variation of the aging rate

One of the more complex aspects of battery performance is the rate at which a battery's capacity and performance degrade over time. The spread of this aging rate across different cells is a critical consideration in battery design and management. However, the factors influencing this spread and the extent to which it can be controlled or mitigated remain unclear. A significant point of contention is whether the aging rate spread can be influenced by selection or usage [31].

The selection process, much like the initial capacity and resistance selection, could potentially be designed to favor cells that exhibit slower aging rates. Alternatively, specific usage patterns or management strategies could be implemented to reduce the aging rate in certain cells. However, these possibilities remain largely theoretical due to a lack of substantial empirical evidence. The available literature does not provide adequately large or comprehensive tests that would allow for a definitive observation of trends in aging rate spread. Therefore, drawing definitive conclusions about the influence of selection or usage on aging rate variability remains challenging.

That said, it is clear that differences exist between cell types and cell chemistries. Different battery chemistries, for instance, have been observed to age at different rates due to their unique electrochemical properties [32]. Similarly, the design and manufacturing processes of different cell types can also influence their aging behavior.

The influence of a spread in aging rate was investigated in simulations 3 and 4. The resulting distribution of cell capacity during the simulation can be seen in Fig. 6. The distribution of cell capacities does not follow a normal distribution, instead resembling a Weibull distribution. Cells that exhibit a high aging rate lose capacity quickly and are exposed to higher cycle depths, leading to even higher aging rates. This results in some cells rapidly losing their capacity, creating a long tail on the lower side of the capacity distribution. As in the previous simulations, a higher initial variance is amplified during the simulation and leads to even higher capacity variations between the aged cells.

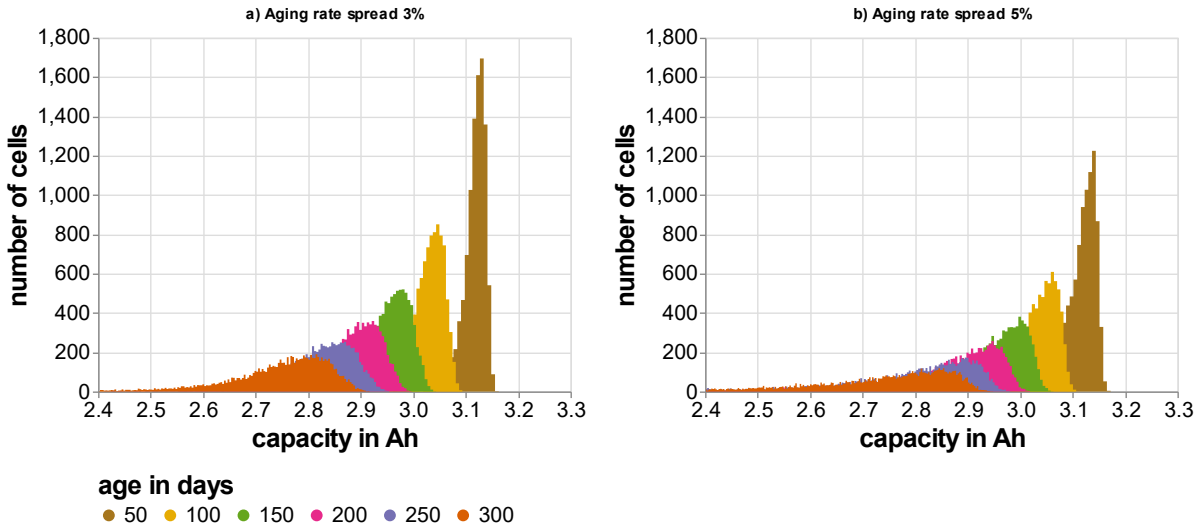

Figure 6: Evolution of the distribution of cell capacity during aging with a variability of aging rate. a) Simulation 3 b) Simulation 4

Variation of the application profile

The usage scenarios of an electric vehicle can significantly influence battery performance and lifespan, with driving habits, charging behaviors, and environmental conditions playing crucial roles. Aggressive driving with rapid acceleration, high speeds, and frequent hard braking can lead to deeper battery discharging and faster degradation, while conservative driving habits can help prolong battery life. Charging behaviors also impact battery health, with frequent fast charging generating more heat and stressing the battery, while slower charging methods and maintaining the state of charge (SOC) between 20% and 80% are less detrimental [23].

Influencing these factors involves a combination of smart charging systems, efficient battery management systems, and features like eco-driving modes. Additionally, the use of telematics and advanced analytics can monitor battery health in real-time and provide feedback to drivers, encouraging more battery-friendly driving and charging habits. This understanding and influencing of usage scenarios is, therefore, a critical aspect of EV design and management.

To investigate the effect of a variation in the application profile, the current profile supplied to the simulation was varied in simulations 5 and 6. The capacity of the cells during the aging simulation can be seen in Fig. 7. As the current is always the same for all 100 cells of one pack, and no cell parameters were varied in these simulations, the cell capacities accumulate at discrete values.

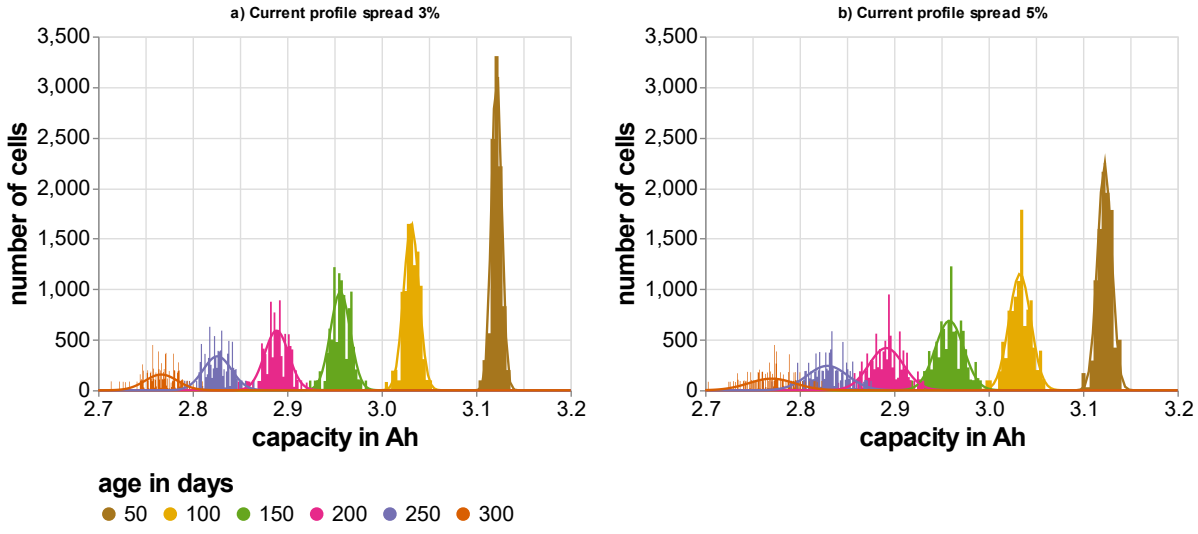

Figure 7: Evolution of the distribution of cell capacity during aging with a variability of the application profile. a) Simulation 5 b) Simulation 6

Combination of parameter variations

In real scenarios, variations of multiple parameters occur simultaneously. The simulation also allows a variability of all investigated parameters at the same time. This was conducted in simulations 7 and 8. The results from these simulations are shown in Fig. 8.
The results show a superposition of all effects observed in the previous simulations. The variation in aging rate leads to capacity distributions that are skewed towards lower values, but this effect is less pronounced due to the influence of the other parameter variations.

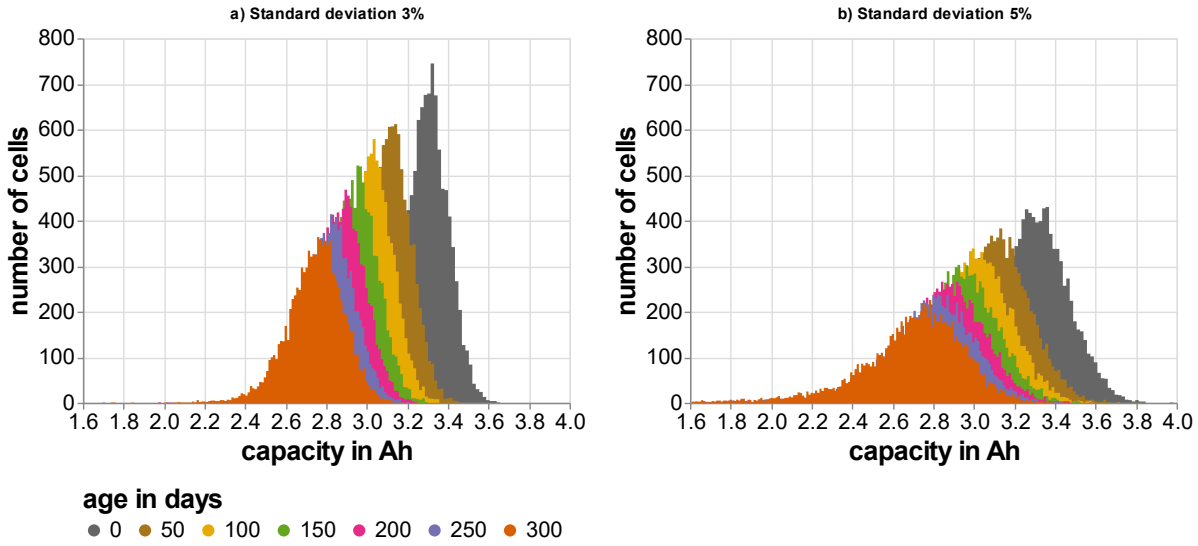

Figure 8: Evolution of the distribution of cell capacity during aging with a combination of the different parameter variations. a) Simulation 7 b) Simulation 8

The results from these simulations show that the different parameter variations compound to create nontrivial spreads in aging behavior that can only be estimated by utilizing a complete battery model like the one presented in this work. The precise modeling of these variations is crucial, as a small variation in initial parameters can increase over time and lead to significant differences in simulation results.

Comparison of different topologies

The lifetime of a battery pack is influenced by various factors, and among the most significant is the interconnection of cells or the pack's topology. Battery pack topology refers to how individual cells are arranged and connected within the battery system. This arrangement doesn't just determine the overall capacity and voltage of the pack; it also shapes the distribution of electrical and thermal loads across the cells, thereby influencing the pack's aging behavior.

When cells are connected in parallel, the current is distributed among individual cells based on their impedance. Consequently, cells that have aged more significantly, and thus have a higher internal resistance, are subject to lower current and experience reduced charge throughput. This inherent balancing effect between stronger and weaker cells can enhance the overall battery pack's lifetime [9].

However, there is no universal solution when it comes to pack topologies, and commercial battery packs exhibit a broad range of parallel and series configurations of cells with large differences in the capacity of a single cell. This vast diversity in design underscores the necessity for an investigation into how different pack topologies impact battery aging.

Simulations 9 and 10 were performed with pack topologies that include parallel connections and a combination of all 3 parameter variations. Fig. 9 shows the distribution of cell capacity after 300 days along with the results for the 100s1p topology previously simulated in simulation 7. It can be seen that the topology has a slight influence on the capacity of the aged cells, with parallel interconnections leading to higher remaining capacities. Additionally, the variance in cell capacities is smaller for parallel topologies, as the cells connected in parallel lead to an equalization effect and thus to more uniform aging rates.

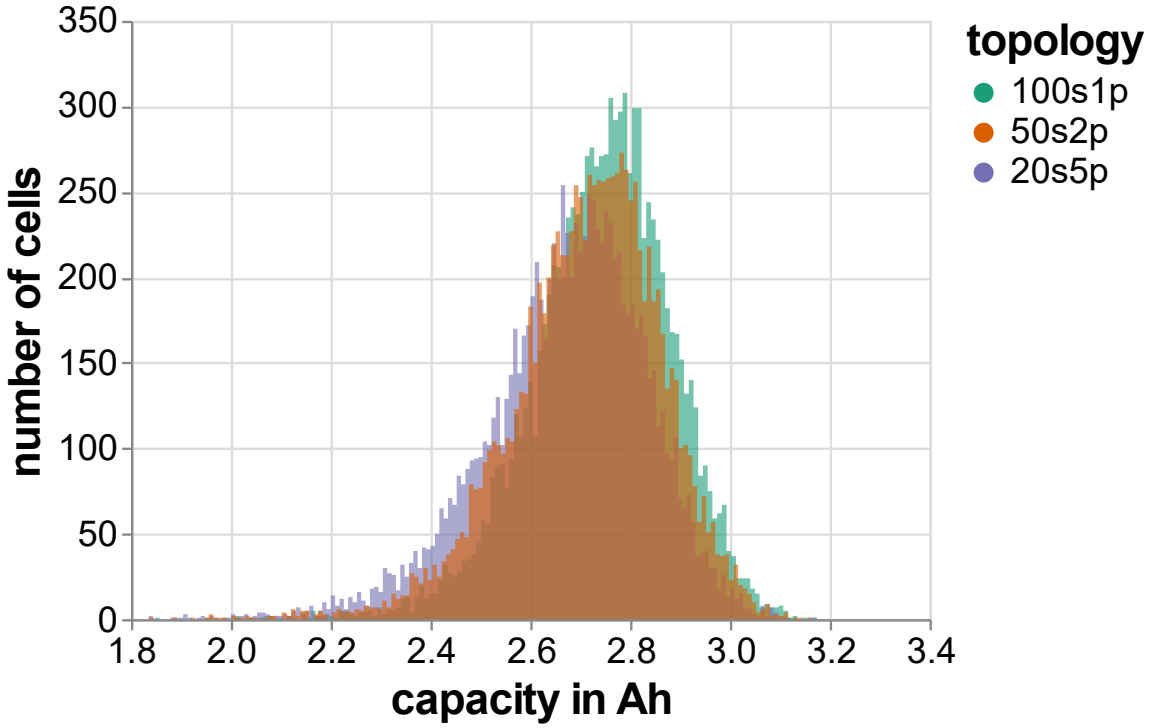

Figure 9: Distribution of the cell capacities after aging for different topologies.

Time to end-of-life

To determine the implications of variabilities in aging on the design and operation of batteries, it is crucial to study the effect on lifetime, as this determines the cost and feasibility of the entire battery system. To this end, it is possible to calculate for each cell after what time it will reach the end of its lifetime. For this purpose, the time at which 80% of the nominal capacity is still present is used. In the simulation, an aging step is performed every 10 days, in which the new capacity of the cells is calculated. In order to determine the lifetime to the day, the capacity is therefore linearly interpolated between the aging steps. This calculation can be used to derive a histogram of cell lifetimes, as is illustrated in Fig. 10. The relative capacity shown in this figure is calculated based on the nominal cell capacity.

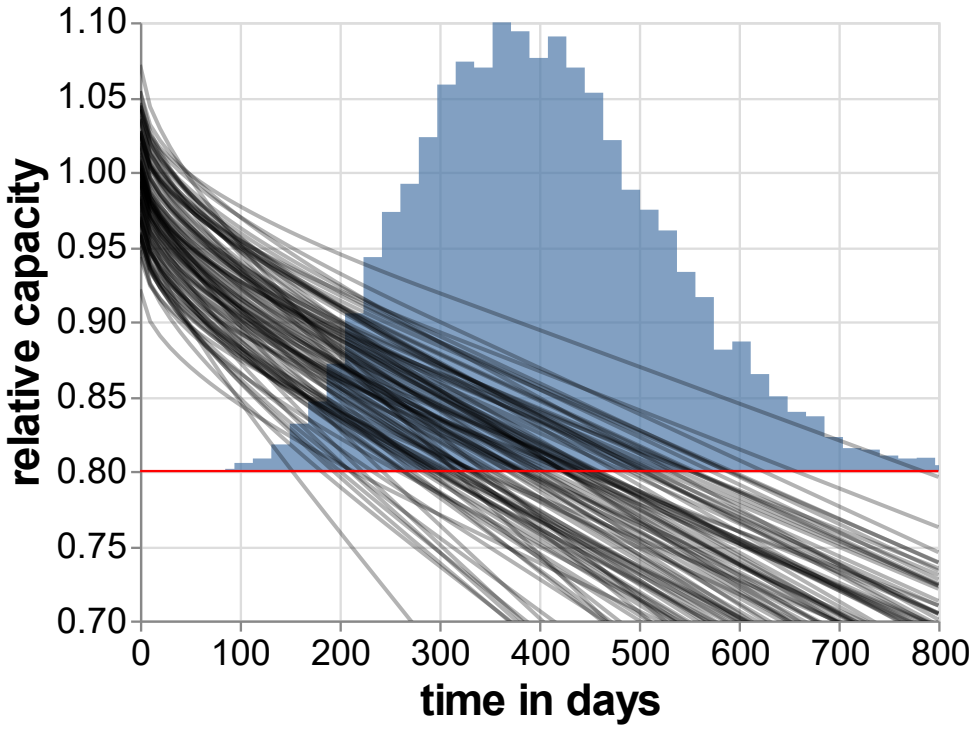

Figure 10: Calculation of cell lifetime from capacity trends. The red line shows the end-of-life criterion at 80%. The intercept of a degradation curve with the end-of-life criterion is shown in the histogram.

The achieved lifetime of the simulated cells in simulations 7, 9, and 10 can be seen as a histogram for all topologies in Fig. 11. The lifetime shows the largest variability for the series connection and gets more uniform the more cells are connected in parallel. The average cell lifetime depends on the battery pack topology and increases with added parallel connections.

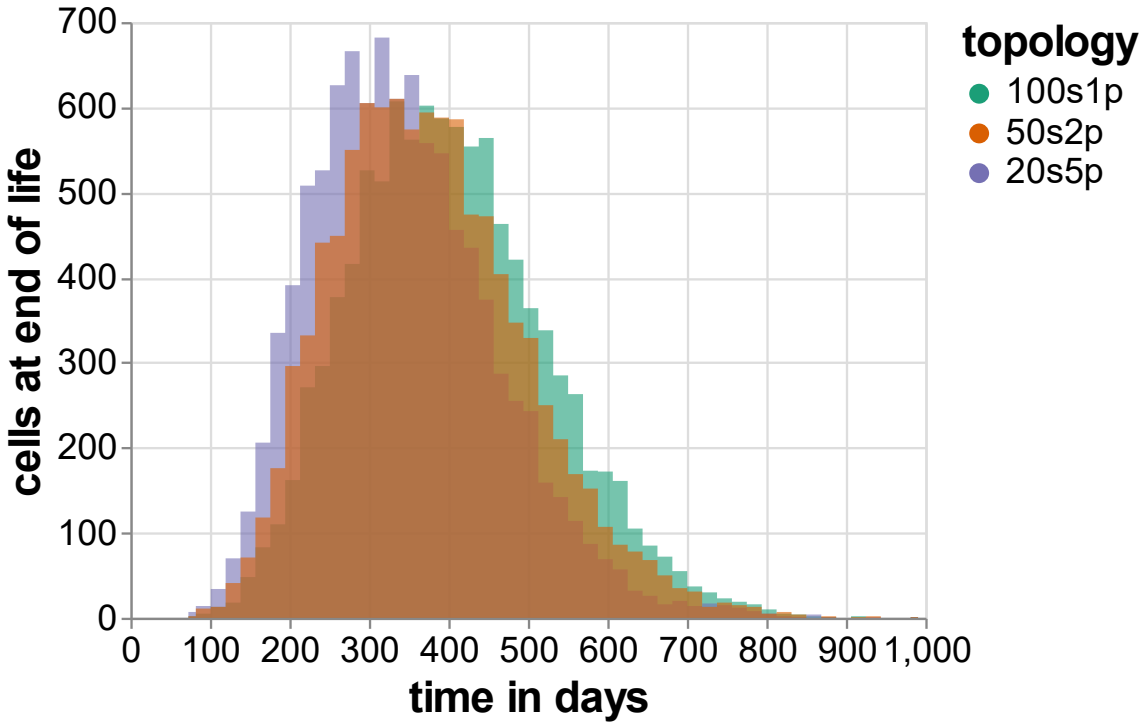

Figure 11: Effect of topology on cell life.

The lifetime can also be determined for the entire battery pack. In the series connection, the lifetime of the pack is equal to the lifetime of the earliest failing cell. In parallel connection, the capacity of the cells connected in parallel is averaged. As soon as the average capacity of a parallel connection falls below 80% of the nominal cell capacity, the lifetime of the entire pack ends. The lifetimes of the battery packs calculated in this way can be seen in Fig. 12.

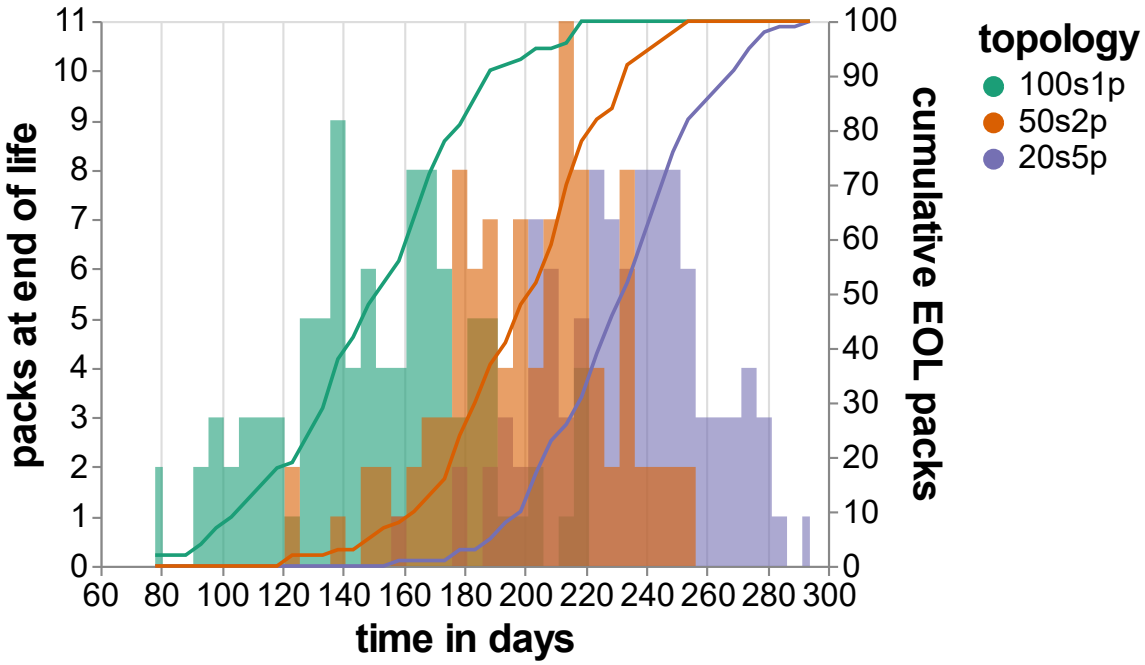

Figure 12: Effect of topology on battery pack lifetime.

Although the cell lifetimes are similar for the three topologies, the pack lifetimes are very different. Since in the serial connection, the worst cell determines the end of life of the pack, with the first cells failing between 80 and 100 days, also the first packs of the 100s1p pack topology start to fail. After that, the 50s2p topology can be found in the middle, with packs failing from 120 to 240 days. The other packs, with the five parallel cells, start to fail last at around 160 days.

Influence of cell-to-cell variation on pack lifetime

In order to further investigate how the pack topology affects the level of variation between cells that is acceptable for the application, additional simulations were conducted to compare the pack lifetime for different levels of cell-to-cell variations in topologies with and without parallel connections.

This represents the choice between using large cells that are only connected in series, or smaller cells that are used in parallel to increase their capacity. Using larger cells can have advantages for the manufacturer, but since there is no equalization between stronger and weaker parallel cells, a higher homogeneity is required to achieve the same performance and lifetime.

In simulations 11 and 12, a 100s10p topology was simulated with two levels of parameter variations. The simulations 13 to 22 show the impact of the level of cell-to-cell variation in a series configuration by simulating a 100s1p topology with variations increasing from 0.5% to 5% in 0.5% steps.

For all simulations, the lifetime of each battery pack was evaluated based on the same 80% capacity criterion used above. Figure 13 shows the cumulative number of packs that have reached the end of their life for each of the 12 simulations.

The results show a clear difference between the two topologies, with the 100s10p topology having a significantly longer lifetime for the same amount of variation between the individual cells. This shows that a higher homogeneity between cells is needed for cells used in a series configuration in order to achieve the same performance and lifetime that would be possible with paralleled cells.

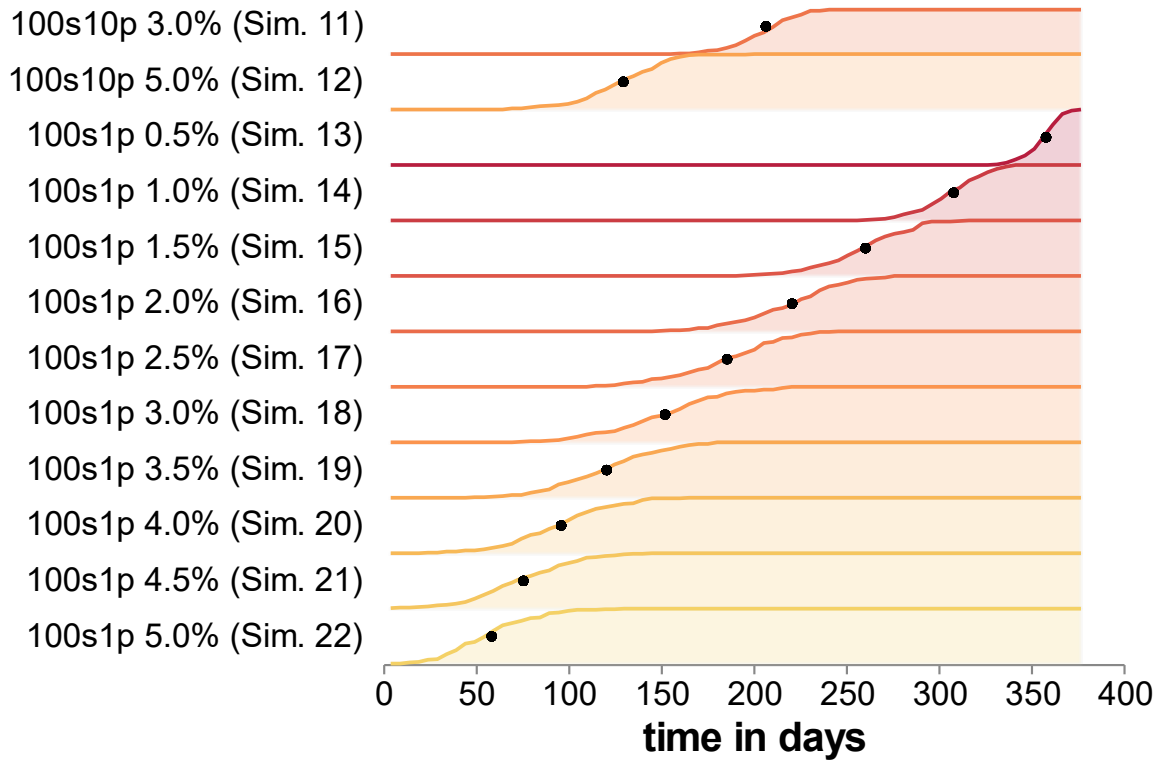

Figure 13: Effect of the level of cell-to-cell variation on the lifetime of the battery pack. The average pack lifetime for each simulation is marked with a black dot.

Conclusion

A modeling framework was created to mimic the electrical, thermal, and aging behavior of batteries in various configurations based on an impedance-based cell model. Batteries may be simulated several times as part of a Monte Carlo simulation using load profiles, consumption patterns, and lifespan needs, with cell attributes generated from the aging rate distributions and initial spread distributions. Given a specific topology and distribution, it is possible to determine the degradation of each cell inside the battery as well as the number of failed cells and failed packs, allowing for "fleet-level" comparisons. This not only helps in simulating the expected life of a battery but also enables the investigation of failure distributions, which is essential for financial risk assessment and safety considerations in electric vehicle design. A comparison between topologies with and without parallel connections shows a significantly larger impact of cell-to-cell variations on packs with only serial connections, showing that more homogenous cells are required for usage in packs with these topologies.

In conclusion, our work has provided valuable insights into the stochastic simulation of varying battery aging behavior and highlighted the importance of accurately characterizing cell-to-cell variability for practical applications. We have also demonstrated the limitations of current experimental designs and emphasized the need to develop more reliable and robust designs for battery aging tests that can capture the inherent variability of the aging process. Such designs will not only improve our understanding of battery aging, but also enable the development of more efficient and durable battery technologies for a wide range of applications.

Acknowledgements:

This work was financially supported by the German Federal Ministry of Education and Research within the SimBAS project (Grant No. 03XP0338B) and the BALd project (Grant No. 03XP0320A), managed by Project Management Jülich. The responsibility for this publication rests with the authors.

Conflict of Interest

The authors declare no conflict of interest.

CRediT Author Contributions Statement

E.B.: conceptualisation, methodology, software, data curation, writing – original draft, visualization.
F.H. software, methodology.
F.E.A.H.: methodology, writing – review and editing.
F.F: methodology, data curation, writing – review and editing.
K.Q: data curation, writing – review and editing.
S.B.: software, data curation, writing – review and editing.
D.U.S.: methodology, supervision, funding acquisition.
P.D.: conceptualisation, methodology, software, data curation, writing – original draft, visualization, supervision.

Disclaimer on the use of AI writing aids:

During the preparation of the manuscript the authors used GPT4/OpenAI in order to improve readability and language. After using this tool, the authors reviewed and edited the content as needed and take full responsibility for the content of the publication.

References:

[1] P. Dechent *et al.*, “Correlation of Health Indicators on Lithium-Ion Batteries,” *Energy Technology*, p. 2201398, doi: 10.1002/ente.202201398.
[2] D. Beck, P. Dechent, M. Junker, D. U. Sauer, and M. Dubarry, “Inhomogeneities and Cell-to-Cell Variations in Lithium-Ion Batteries, a Review,” *Energies*, vol. 14, no. 11, p. 3276, Jun. 2021, doi: 10.3390/en14113276.
[3] S. Paul, C. Diegelmann, H. Kabza, and W. Tillmetz, “Analysis of ageing inhomogeneities in lithium-ion battery systems,” *Journal of Power Sources*, vol. 239, pp. 642–650, Oct. 2013, doi: 10.1016/j.jpowsour.2013.01.068.
[4] K. Rumpf, M. Naumann, and A. Jossen, “Experimental investigation of parametric cell-to-cell variation and correlation based on 1100 commercial lithium-ion cells,” *Journal of Energy Storage*, vol. 14, no. Part 1, pp. 224–243, Dec. 2017, doi: 10.1016/j.est.2017.09.010.
[5] M. Schindler, J. Sturm, S. Ludwig, J. Schmitt, and A. Jossen, “Evolution of initial cell-to-cell variations during a three-year production cycle,” *eTransportation*, p. 100102, Jan. 2021, doi: 10.1016/j.etran.2020.100102.
[6] S. J. Harris, “Failure statistics for commercial lithium ion batteries: A study of 24 pouch cells,” *Journal of Power Sources*, p. 9, 2017.
[7] T. Baumhöfer, M. Brühl, S. Rothgang, and D. U. Sauer, “Production caused variation in

capacity aging trend and correlation to initial cell performance," *Journal of Power Sources*, p. 7, 2014.
[8] J. M. Reniers and D. A. Howey, "Digital twin of a MWh-scale grid battery system for efficiency and degradation analysis," *Applied Energy*, vol. 336, p. 120774, Apr. 2023, doi: 10.1016/j.apenergy.2023.120774.
[9] M. Dubarry, C. Pastor-Fernández, Carlos, G. Baure, T. F. Yu, W. D. Widanage, and J. Marco, "Battery energy storage system modeling: Investigation of intrinsic cell-to-cell variations," *Journal of Energy Storage*, vol. 23, pp. 19–28, 2019, doi: 10.1016/j.est.2019.02.016.
[10] Y. Zhang, R. Xiong, H. He, and M. G. Pecht, "Lithium-Ion Battery Remaining Useful Life Prediction With Box–Cox Transformation and Monte Carlo Simulation," *IEEE Trans. Ind. Electron.*, vol. 66, no. 2, pp. 1585–1597, Feb. 2019, doi: 10.1109/TIE.2018.2808918.
[11] A. Fill, D. Müller, and K. P. Birke, "Influence of the Cell Topology, Thermal Conditions and initial Cell to Cell Variances on Aging Gradients among Lithium-Ion Cells of a Battery," in *2021 IEEE 15th International Conference on Compatibility, Power Electronics and Power Engineering (CPE-POWERENG)*, Jul. 2021, pp. 1–8. doi: 10.1109/CPE-POWERENG50821.2021.9501074.
[12] "ISEAFrame," *GitLab, RWTH Aachen University*, Dec. 31, 2022. https://git.rwth-aachen.de/isea/framework (accessed May 19, 2023).
[13] F. E. Hust, "Physico-chemically motivated parameterization and modelling of real-time capable lithium-ion battery models : a case study on the tesla model s battery," *RWTH Aachen University*, 2018, doi: 10.18154/RWTH-2019-00249.
[14] F. Hildenbrand, D. Ditscheid, E. Barbers, and D. U. Sauer, "Influence of the anode overhang on the open-circuit voltage and the ageing of lithium-ion batteries—A model based study," *Applied Energy*, vol. 332, p. 120395, Feb. 2023, doi: 10.1016/j.apenergy.2022.120395.
[15] H. Witzenhausen, "Elektrische Batteriespeichermodelle: Modellbildung, Parameteridentifikation und Modellreduktion," PhD thesis, RWTH Aachen University, Aachen, Germany, 2017. doi: 10.18154/RWTH-2017-03437.
[16] M. Dubarry and B. Y. Liaw, "Development of a universal modeling tool for rechargeable lithium batteries," *Journal of Power Sources*, vol. 174, no. 2, pp. 856–860, Dec. 2007, doi: 10.1016/j.jpowsour.2007.06.157.
[17] L. Zhang, H. Peng, Z. Ning, Z. Mu, and C. Sun, "Comparative Research on RC Equivalent Circuit Models for Lithium-Ion Batteries of Electric Vehicles," *Applied Sciences*, vol. 7, no. 10, p. 1002, Oct. 2017, doi: 10.3390/app7101002.
[18] M. Steinhardt *et al.*, "Low-effort determination of heat capacity and thermal conductivity for cylindrical 18650 and 21700 lithium-ion cells," *Journal of Energy Storage*, vol. 42, p. 103065, Oct. 2021, doi: 10.1016/j.est.2021.103065.
[19] C. R. Birkl, M. R. Roberts, E. McTurk, P. G. Bruce, and D. A. Howey, "Degradation diagnostics for lithium ion cells," *Journal of Power Sources*, vol. 341, pp. 373–386, Feb. 2017, doi: 10.1016/j.jpowsour.2016.12.011.
[20] M. Lewerenz, G. Fuchs, L. Becker, and D. U. Sauer, "Irreversible calendar aging and quantification of the reversible capacity loss caused by anode overhang," *Journal of Energy Storage*, vol. 18, pp. 149–159, Aug. 2018, doi: 10.1016/j.est.2018.04.029.
[21] J. M. Reniers, G. Mulder, and D. A. Howey, "Review and Performance Comparison of Mechanical-Chemical Degradation Models for Lithium-Ion Batteries," *J. Electrochem. Soc.*, vol. 166, no. 14, pp. A3189–A3200, Jan. 2019, doi: 10.1149/2.0281914jes.
[22] J. Schmalstieg, S. Käbitz, M. Ecker, and D. U. Sauer, "A holistic aging model for Li(NiMnCo)O2 based 18650 lithium-ion batteries," *Journal of Power Sources*, vol. 257, pp. 325–334, Jul. 2014, doi: 10.1016/j.jpowsour.2014.02.012.
[23] M. Ecker, "Calendar and cycle life study of Li(NiMnCo)O2-based 18650 lithium-ion batteries," *Journal of Power Sources*, vol. 248, pp. 839–851, 2014, doi: 10.1016/j.jpowsour.2013.09.143.
[24] S. Käbitz *et al.*, "Cycle and calendar life study of a graphite|LiNi1/3Mn1/3Co1/3O2 Li-ion high energy system. Part A: Full cell characterization," *Journal of Power Sources*, vol.

239, pp. 572–583, Oct. 2013, doi: 10.1016/j.jpowsour.2013.03.045.
[25] M. Dubarry and G. Baure, “Perspective on Commercial Li-ion Battery Testing, Best Practices for Simple and Effective Protocols,” *Electronics*, vol. 9, no. 1, Art. no. 1, Jan. 2020, doi: 10.3390/electronics9010152.
[26] M. Ecker *et al.*, “Development of a lifetime prediction model for lithium-ion batteries based on extended accelerated aging test data,” *Journal of Power Sources*, vol. 215, pp. 248–257, Oct. 2012, doi: 10.1016/j.jpowsour.2012.05.012.
[27] S. J. Harris and M. M. Noack, “Statistical and machine learning-based durability-testing strategies for energy storage,” *Joule*, vol. 7, no. 5, pp. 920–934, Apr. 2023, doi: 10.1016/j.joule.2023.03.008.
[28] I. Zilberman, S. Ludwig, and A. Jossen, “Cell-to-cell variation of calendar aging and reversible self-discharge in 18650 nickel-rich, silicon–graphite lithium-ion cells,” *Journal of Energy Storage*, vol. 26, p. 100900, Dec. 2019, doi: 10.1016/j.est.2019.100900.
[29] J. Becker, T. Nemeth, R. Wegmann, and D. U. Sauer, “Dimensioning and Optimization of Hybrid Li-Ion Battery Systems for EVs,” *World Electric Vehicle Journal*, vol. 9, no. 2, p. 19, Jun. 2018, doi: 10.3390/wevj9020019.
[30] T. Nemeth, A. Bubert, J. N. Becker, R. W. D. Doncker, and D. U. Sauer, “A Simulation Platform for Optimization of Electric Vehicles With Modular Drivetrain Topologies,” *IEEE Transactions on Transportation Electrification*, vol. 4, no. 4, pp. 888–900, Dec. 2018, doi: 10.1109/TTE.2018.2869371.
[31] M. Baumann, L. Wildfeuer, S. Rohr, and M. Lienkamp, “Parameter variations within Li-Ion battery packs – Theoretical investigations and experimental quantification,” *Journal of Energy Storage*, vol. 18, pp. 295–307, Aug. 2018, doi: 10.1016/j.est.2018.04.031.
[32] Y. Preger *et al.*, “Degradation of Commercial Lithium-Ion Cells as a Function of Chemistry and Cycling Conditions,” *J. Electrochem. Soc.*, vol. 167, no. 12, p. 120532, Sep. 2020, doi: 10.1149/1945-7111/abae37.
[33] M. Dubarry, C. Truchot, and B. Y. Liaw, “Synthesize battery degradation modes via a diagnostic and prognostic model,” *Journal of Power Sources*, vol. 219, pp. 204–216, Dec. 2012, doi: 10.1016/j.jpowsour.2012.07.016.
[34] M. Dubarry, “Big data training data for artificial intelligence-based Li-ion diagnosis and prognosis,” *Journal of Power Sources*, vol. 479, p. 228806, 2020, doi: 10.1016/j.jpowsour.2020.228806.